

## Highly Accurate and Cost-effective Auto-tracking Antenna System for Satellite Broadband Communication on Vessels

*Tomihiko Yoshida<sup>†</sup>, Kohei Ohata, and Masazumi Ueba*

### Abstract

At the World Radiocommunication Conference in 2003, ITU-R (International Telecommunication Union Radiocommunication Sector) decided to allow maritime mobile applications to use the frequency band for fixed-satellite services on the condition that the antennas have peak pointing accuracy of  $0.2^\circ$ . However, this level of accuracy is usually achieved only with expensive, highly accurate gyro systems and monopulse antennas. This paper describes a cost-effective shipboard antenna system that complies with the ITU-R requirements. It features a novel inclinometer that is robust against acceleration disturbances and a novel control design process that obtains highly accurate controllers from low-cost sensors. Simulation and experimental results verify that these features make possible an antenna system that meets the ITU-R requirements with a low system cost.

### 1. Introduction

The recent exponential growth of high-speed Internet connections has created a huge demand for ubiquitous access links to the Internet, and mobile Internet services on cellular or wireless LAN networks have increased rapidly. A major role of mobile satellite communication networks is to provide ubiquitous broadband services. The target users of these services are people who do not have access to terrestrial networks, such as passengers on ships, airliners, and trains.

The satellite network we envisage uses the Ku-band (14/12 GHz) and has an onboard antenna diameter of about 1 m to handle broadband services with bit rates of several tens of megabits per second. The Ku-band is primarily allocated to fixed satellite services, so the transmitting antenna system must have the same pointing accuracy as fixed earth stations. ITU-R<sup>\*1</sup> established the technical constraints on the pointing errors and other antenna attributes for earth stations onboard vessels (ESVs) in WRC<sup>\*2</sup> 2003 [1]. The antenna pointing error of the mobile terminals in narrowband systems for mobile satellite services, such

as Inmarsat [2], is a few degrees [3]. In contrast, the pointing accuracy requirement for ESV antennas is  $0.2^\circ$  peak [1], one order of accuracy higher. This level of accuracy usually demands extremely accurate sensors, such as ring laser gyros (RLGs), which greatly increase the antenna system costs.

There have been very few studies on shipboard antenna systems that can accommodate the ITU-R restrictions at a relatively low cost. Taylor [4] uses two mechanical gyros to stabilize the antenna platform. The basic principle of stabilization is that the inertial wheel can maintain a constant direction while the ves-

<sup>\*1</sup> ITU-R: International Telecommunication Union Radiocommunication Sector. ITU-R is the radiocommunication sector in ITU. It allocates bands of the radio-frequency spectrum, allots radio frequencies, and registers radio-frequency assignments of any associated orbital position in the geostationary satellite orbit to avoid harmful interference between radio stations of different countries. It also coordinates efforts to eliminate harmful interference between radio stations of different countries and improve the use made of radio frequencies and of the geostationary satellite orbits for radiocommunication services (<http://www.itu.int/ITU-R/>).

<sup>\*2</sup> WRC: World Radiocommunication Conference. WRCs are held every two to three years. It is the job of WRC to review, and, if necessary, revise the Radio Regulations, the international treaty governing the use of the radio-frequency spectrum and the geostationary and non-geostationary satellite orbits. Revisions are made on the basis of an agenda determined by the ITU Council, which takes into account recommendations made by previous world radiocommunication conferences.

<sup>†</sup> NTT Access Network Service Systems Laboratories  
Yokosuka-shi, 239-0847 Japan  
E-mail: yoshida.tomihiko@lab.ntt.co.jp

sel moves. However, we would need an inertial wheel that can withstand  $10 \text{ kg}\cdot\text{m}^2$  (diameter: 1 m, weight: 80 kg) at 6600 rpm for the stabilizer to be applicable to our new antenna system. This makes the system impractically large and heavy. Dang et al. applied an electronic beam-squint tracking system [5], [6] to an antenna feed. They used an improved single-horn feed, using electronic beam-squint tracking. In spite of using the single-horn feed, this tracking system has almost the same tracking accuracy as a monopulse (multi-horn) system. However, it requires a large-aperture antenna to achieve accurate tracking. The prototype has a 2.4-m antenna for the Ku-band.

This paper describes a highly accurate and cost-effective auto-tracking antenna system for ESVs. The antenna diameter is about 1 m [7]. To reduce the system cost, we used a combination of low-cost commercial sensors. The key features are the system configuration, an inclinometer that is robust against acceleration disturbances, and a control design process that obtains highly accurate controllers. These are described in sections 3, 4, and 5, respectively.

## 2. Requirements

The roll and pitch of a vessel are very important conditions in the design of the controller. Lucke et al. [8] investigated the dynamic motions of a 150-m ferryboat. They showed that the maximum angle was  $3^\circ$ , and the strongest motion appeared at about 0.1 Hz, at a speed of 18 knots. We set more severe conditions and observed them on a vessel with a displacement of a few thousand tons under stormy weather conditions. The system was required to have an antenna pointing accuracy of  $0.2^\circ$  peak to meet the ITU-R

requirements under the following conditions:

- 1) Attitude angle of vessel: (worst conditions)  
 $10^\circ$  maximum at 0.1 Hz (angular rate:  $6^\circ/\text{s}$  at 0.1 Hz)
- 2) Vessel acceleration:  
 $0.05 \text{ m/s}^2$  during 300 s (maximum speed: 30 knots)
- 3) Antenna aperture diameter:  
 1 m (typical value; in practice, it depends on the link budget design.)

## 3. Antenna system configuration

To reduce the system cost and achieve high pointing accuracy, we selected the most suitable mechanical configuration and sensors as follows.

### 3.1 Mechanical configuration

A shipboard antenna system needs two types of control: 1) a stabilization control [4] to compensate for the vessel's dynamic motion by using attitude sensors, such as gyros and 2) a tracking control [5] to orientate the antenna by sensing the received signal. For the stabilization control, we selected a stable platform configuration [9] so that we could use moderately accurate sensors, such as a fiber optical gyro (FOG) to reduce costs [7]. Stable platform systems usually have a 3- or 4-axis antenna mount [4], [10], as shown in **Fig. 1**. The 4-axis mount (Fig. 1(b)) consists of a 2-axis leveling platform as the stable platform and a 2-axis antenna pointing mechanism (APM) on the leveling platform. The 3-axis mount (Fig. 1(a)) treats the antenna as the stable platform. Although the 4-axis mount is mechanically more complex than the 3-axis mount, its controller has a simpler design because the

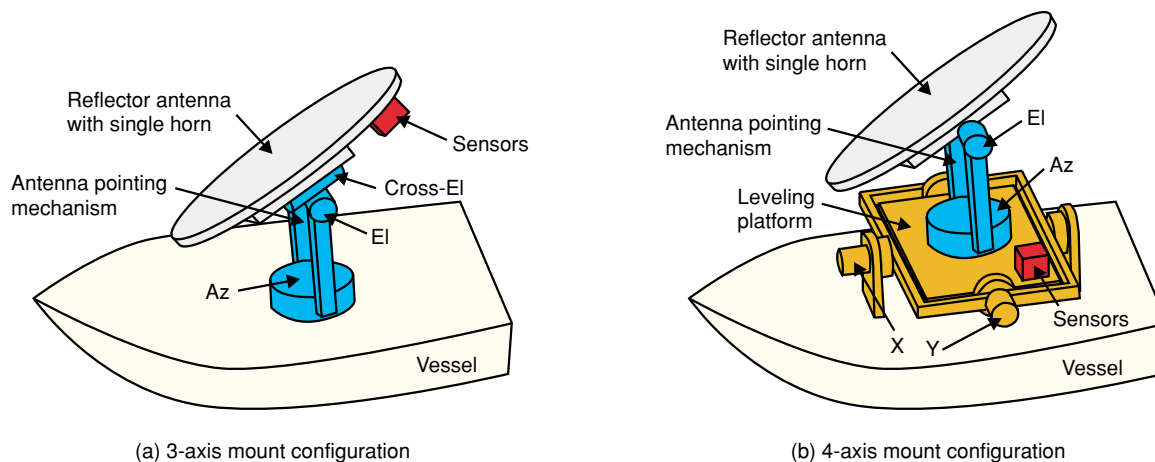


Fig. 1. Antenna mount configurations for stable platform systems.

stabilization and tracking controllers can be designed independently, while the controller for the 3-axis mount must integrate reciprocal functions, such as stabilization and tracking, on each axis.

### 3.2 Sensors

For tracking control, we used an ordinary reflector antenna with a single horn. Many radar systems use a monopulse antenna [11], which has a set of feed horns [12]. This type of antenna can detect the pointing error angle and direction instantaneously from the phase or amplitude differences of the received signals in each feed. This capability is well suited to accurate tracking control. However, monopulse horns are expensive and can be used only if the antenna's aperture diameter is equal to a few hundred times the wavelength ( $\lambda = 25 \text{ mm}$  at 12 GHz) because the multiple horn configurations degrade the antenna pattern. Our target is ESV antennas with a reflector diameter of less than  $40 \lambda$  (1 m). Therefore, a monopulse antenna is inappropriate for our system. On the other hand, a single horn antenna (SHA) cannot directly detect the pointing error angle and direction. The pointing error is detected by comparing the signal levels of the neighboring angles, using what is called a step-track technique [13]. The sensitivity against pointing errors is low around the target direction because the antenna has a round-shaped peak pattern. Modulation makes the signal level unstable, and background noise wors-

ens it. All these factors make it difficult to achieve agile tracking control using an SHA, so highly accurate stabilization control is needed.

For stabilization control, we used an FOG instead of highly accurate, but expensive gyros such as RLGs. While FOG is a cost-effective gyro, it has a considerable drift error (low frequency bias fluctuation) of almost a few degrees per hour. Therefore, FOGs are basically used for inclinometer combinations, such as accelerometers, to compensate for low-frequency drift errors. Unfortunately, this combination cannot compensate for low-frequency acceleration disturbances when the vessel starts, stops, or turns (note that these accelerations sometimes continue for several minutes). The biggest challenge we faced was to provide a solution to that issue by introducing the inclinometer shown in section 4 to satisfy the antenna system's pointing accuracy requirements.

### 3.3 Antenna system

Based on these considerations, we chose the 4-axis antenna system shown in Fig. 1(b). The antenna system consists of a leveling platform with an X-Y pedestal, an APM with an Az-EI pedestal on the leveling platform, and an SHA on the APM. As sensors, a dual-axis FOG and inclinometers were placed on the leveling platform, and a single-axis FOG was mounted on the Az-axis of the APM. A block diagram of the total antenna system model is shown in Fig. 2.

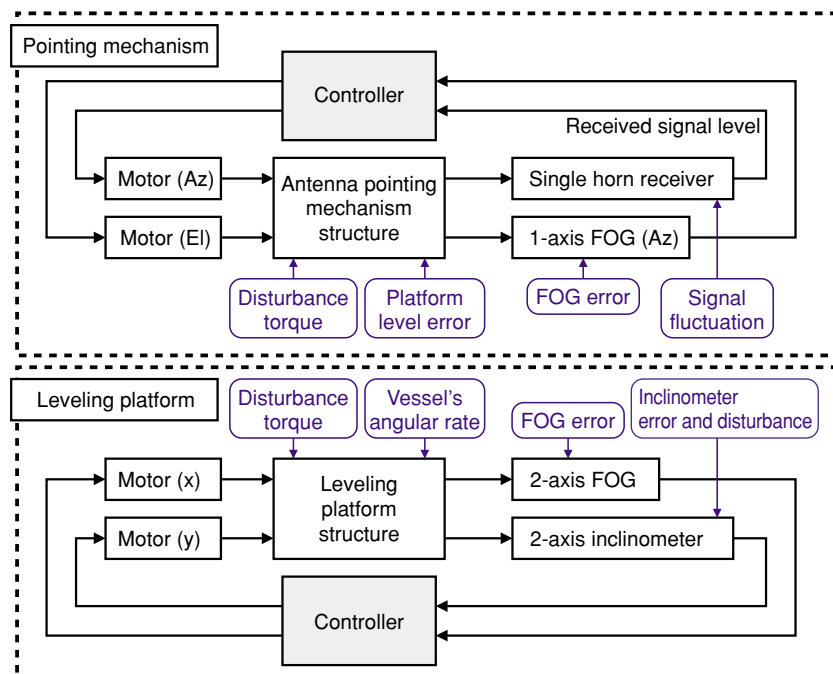


Fig. 2. Block diagram of antenna system.

### 4. Inclinometer

Basically, almost all conventional inclinometers sense the level/angle based on gravity. Therefore, conventional inclinometers cannot be used to estimate accurate level/angles under acceleration disturbance conditions. Our inclinometer overcomes this drawback.

#### 4.1 Configuration

The configuration is shown in Fig. 3. The inclinometer consists of a dual-axis accelerometer, a pendulum, and a rotary encoder. The accelerometer and the encoder housing are mounted on the body, and the pendulum is fixed to the encoder axis. The pendulum axis coincides with the encoder axis. The principle of level/angle estimation is described by

$$\theta = \phi - \psi, \tag{1}$$

where  $\theta$  is the level/angle,  $\phi$  is the inertial angle of the pendulum, and  $\psi$  is the relative rotation angle of the encoder, as shown in Fig. 4. Because  $\psi$  is measured

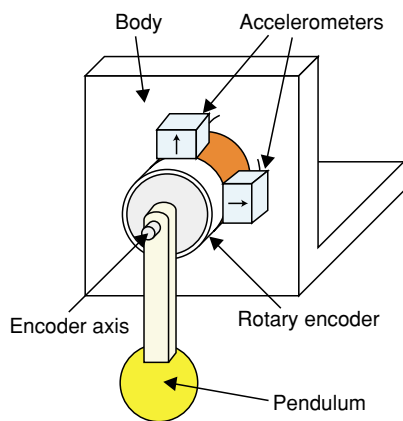


Fig. 3. Inclinometer configuration.

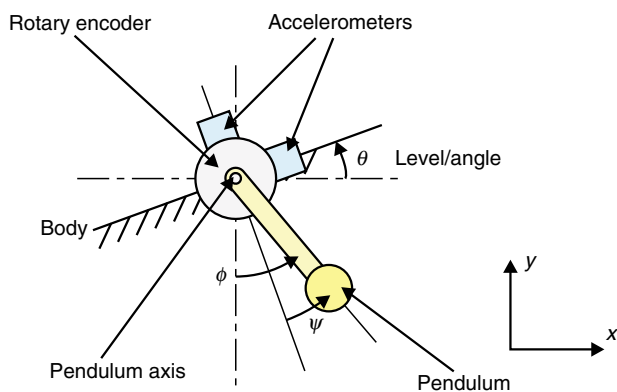


Fig. 4. Principle of level/angle estimation.

directly by the encoder,  $\theta$  can be obtained by estimating  $\phi$ . The distinguishing feature of our inclinometer is that the estimation algorithm uses the pendulum's equation of motion.

#### 4.2 Simulation

The results of a time simulation are shown in Figs. 5 and 6. The assumed level/angle of the moving body was  $10^\circ$  at 0.1 Hz, and the low-frequency disturbances caused by the translational accelerations were 0, 0.2, and  $-0.2 \text{ m/s}^2$  during the time periods 0–100, 100–200, and 200–300 s, respectively. The distance from the rotation center of the moving body to the inclinometer mounting point was 1 m. The assumed model parameter error, which is the inevitable ambiguity in a practical system, was 1%, and the assumed analog/digital converter sampling period was 0.01 s. The results obtained using a conventional inclinometer are shown in Fig. 5; those for our inclinometer are shown in Fig. 6. The upper figures show the estima-

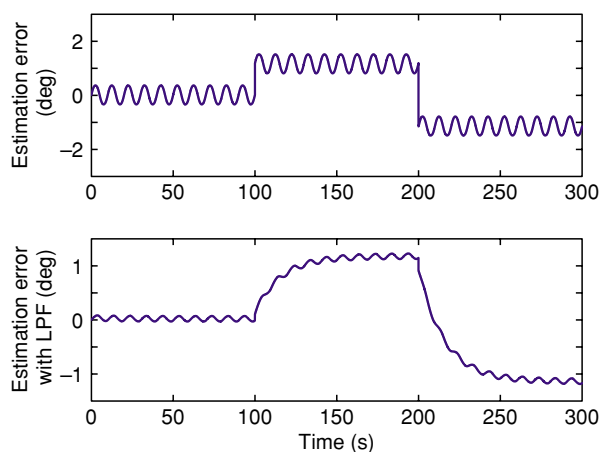


Fig. 5. Estimation errors in a conventional inclinometer.

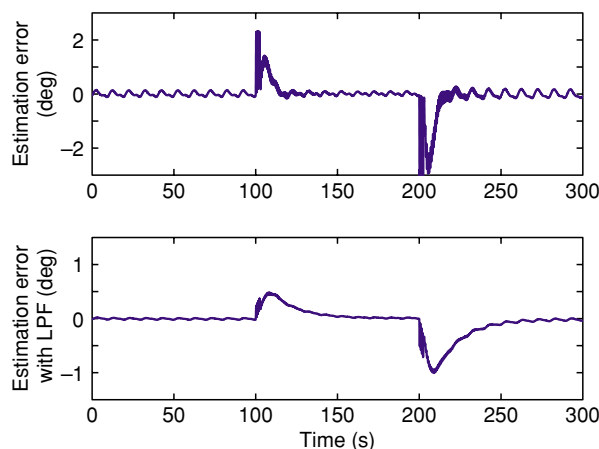


Fig. 6. Estimation errors in our proposed inclinometer.

tion errors, and the lower figures were obtained by applying a 0.01-Hz low-pass filter to the upper results.

The results verify that this inclinometer provided accurate estimations, except for the instant when the acceleration started/finished, while conventional inclinometers were inaccurate throughout the acceleration period because the body acceleration directly affected the level/angle estimation. The simulation results clearly confirm that our inclinometer performed better than the conventional one under acceleration disturbance conditions.

### 4.3 Experimental evaluation

We evaluated the performance of the inclinometer experimentally. The experimental setup of the inclinometer, which comprised a pendulum, a rotary encoder, and accelerometers, is shown in Fig. 7. All the sensors had commercial-quality accuracy. The shaker motion, which was assumed to be the moving body motion, and the resulting level/angle estimation

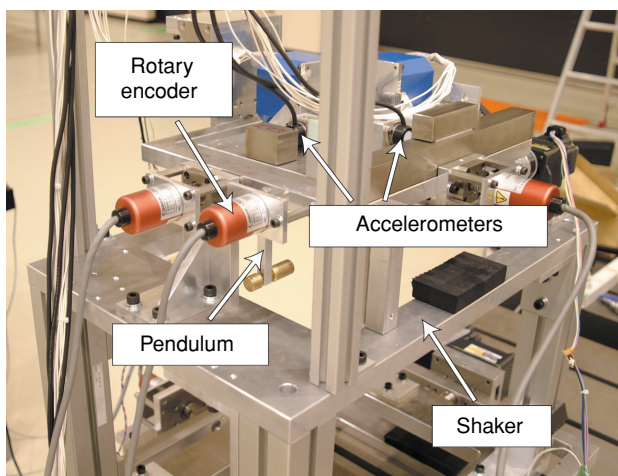


Fig. 7. Experimental equipment for proposed inclinometer.

errors are shown in Fig. 8. These figures verify that the algorithms could provide highly accurate level/angle estimations, especially for low frequencies.

## 5. Controller design

This section describes the design of the controller that can achieve high pointing accuracy using moderately accurate sensors.

### 5.1 Methodology and disturbances

We applied the  $H_\infty$  control [14], [15] to the leveling platform controller design, considering the frequency characteristics of the disturbances. Antenna systems are always affected by disturbances that have frequency characteristics, as shown in Table 1, and are

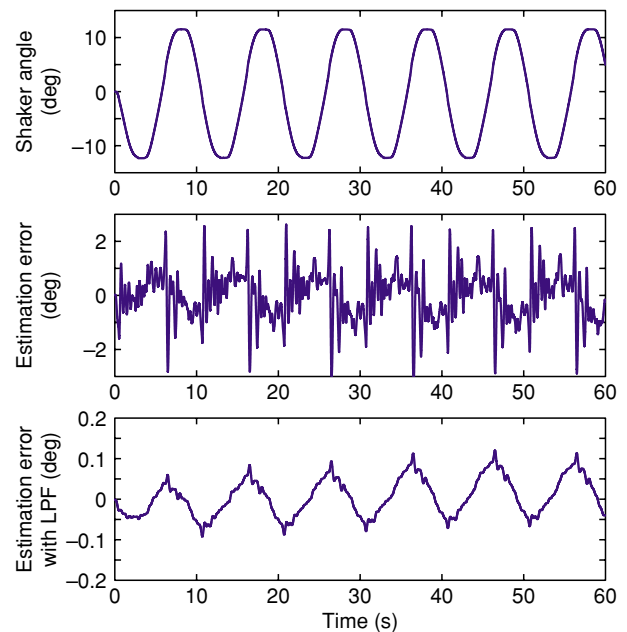


Fig. 8. Shaker angle and estimation errors.

Table 1. Disturbances to leveling platform.

Type	Detail	Freq. band	Maximum value
Disturbance torque	Unbalanced torque	Low	300 kgf-cm (0 Hz)
	Friction, reaction torque from EI axis	Control	
Vessel's angular rate	Angular motion of large vessel	Middle	6°/s (0.1 Hz)
FOG error	Bias fluctuation (offset drift)	Low	0.01°/s ( $2 \times 10^{-3}$ Hz)
	Noise	High	
Accelerometer error and disturbance	Bias, acceleration and turning of vessel	Low	0.05 m/s <sup>2</sup> ( $2 \times 10^{-3}$ Hz)
	Angular motion of large vessel	Middle	
	Noise	High	

Frequency bands: low: 0– $10^{-3}$  Hz, middle:  $10^{-2}$ –1 Hz, high: above 100 Hz, control: 0–10 Hz

generally multi-input multi-output (MIMO) systems, as shown in Fig. 2. Unlike conventional control methods, such as PID (proportional, integral, derivative) that can handle only single-input single-output (SISO) open-loop systems, the  $H_\infty$  control can handle frequency-dependent MIMO closed-loop systems that are impervious to all disturbances. On the other hand,  $H_\infty$  control is unsuitable for APM controllers. Basically,  $H_\infty$  control can be applied to linear systems, but the SHA signal level output does not have a one-to-one relationship with the tracking error angle. Therefore, we designed the platform and APM controllers independently.

## 5.2 Stabilization controller design

### 5.2.1 Controller design process

A highly accurate leveling platform is indispensable, as described in section 3.2. The stabilization controller acts to keep the leveling platform horizontal under the disturbances described in Table 1. No typical controller design process has been demonstrated for  $H_\infty$  control. Thus far, for most controllers, the design processes have depended on the designer's experience and have been tailored to individual systems by trial and error. This generally takes a considerable amount of effort. Our systematic controller design process does not rely on the designer's skill. It also reduces the workload by shortening the repetitive trial-and-error processes.

In  $H_\infty$  control, the weight function is one of the most important parameters in designing the controller because controller performance is highly dependent on the chosen weights. The choice of weights is a trial-and-error process that continues until the required controller performance is obtained. Basically, time simulations are carried out to evaluate the controller performance and this takes a considerable amount of CPU (central processing unit) time. Hence, the cycles of weight function selection and time simulation result evaluation take quite a long time.

We used a double-loop design process that consists of an inner loop and an outer loop, as shown in Fig. 9. The key feature of the process is that the weight functions are almost all designed using the inner-loop process in the full frequency domain. Because  $H_\infty$  control is a design method used in the frequency domain, it is much faster and more efficient to evaluate the frequency characteristics than to evaluate the time simulation, so this greatly improves the design efficiency.

In most cases, the requirements are satisfied by the

inner-loop process alone. In some more difficult cases, such as when there are large disturbance levels with synchronized phases, the control system designed using only the inner-loop process does not meet the requirements. Therefore, the outer-loop process verifies the pointing accuracy through time simulations.

As shown in Fig. 9, the inner-loop process consists of: 1) design of weight functions, 2) derivation of a controller by applying  $H_\infty$  control with weight functions, 3) calculation of open- and closed-loop system characteristics, including the obtained controller, and 4) repetition of steps 1 to 3 until the target gains of the closed-loop system and stability of the open-loop system are both satisfied.

The initial weight functions are also important for reducing the repetitions of the inner loop. They are initially set to the ratio of the maximum value of each disturbance to the controlled output, in this case, the required level/angle. The target gains are set as the ratio of the controlled output to the maximum value of the disturbances. The closed-loop gains obtained in step 3 are required for gains smaller than the target ones.

If the obtained gains do not meet the targets after a

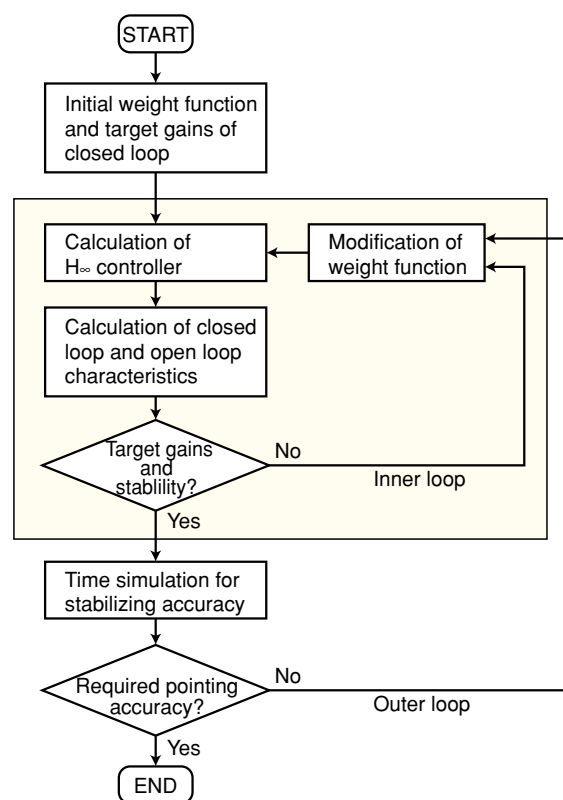


Fig. 9. Controller design process.

few inner-loop iterations, it is likely that no controller can meet the requirements. If this happens, the system configuration or the requirements must be modified. Therefore, this process can also help determine quickly whether or not there is a feasible controller.

We applied the process to the controller design of the leveling platform shown in Fig. 1(b), whose parameters were set to the values for the prototype shown in Fig. 10. The controller’s sampling time was set to 5 ms.

The disturbances are shown in Table 1. The target value of the controlled platform level/angle was  $\pm 0.2^\circ$  ( $\approx \pm 0.0035$  rad). Hence, the target gains of the closed-loop transfer functions are given as follows:

- 1) Disturbance torque to level:  
 $20 \log_{10} (0.0035/300) \approx -100$  dB (0 Hz)
- 2) Angular rate to level:  
 $20 \log_{10} (0.2/6) \approx -30$  dB (0.1 Hz)
- 3) FOG error to level:  
 $20 \log_{10} (0.2/0.01) \approx 26$  dB ( $2 \times 10^{-3}$  Hz)
- 4) Acceleration disturbance to level:  
 $20 \log_{10} (0.0035/(1/9.8)) \approx -30$  dB (0.1 Hz)

After a few repetitions of the inner loop, the obtained gains satisfied the target ones, as shown in



Fig. 10. Antenna system prototype.

**Table 2.** In section 6, we demonstrate that the controller described in this section could achieve the required accuracy.

### 5.2.2 Experimental evaluation

To prove the effectiveness of the design process and confirm the accuracy of the obtained controller, we present experimental results for the leveling platform.

The experimental equipment is shown in Fig. 11. It included a leveling platform mounted on a shaker to simulate the vessel’s angular motion. The actual system size and disturbances are larger than this experimental platform, especially during the platform’s inertial moment, disturbance torque, and acceleration disturbance. Nonetheless, the controller design process is identical to that described in section 5.2.1. The controller used in this experiment was also obtained after executing a few inner-loop repetitions.

The experimental results, shown in Fig. 12, show the level angles of the controlled platform and the motion angle of the shaker. The frequency character-

Table 2. Closed-loop gains after control design process.

Input	Obtained gain	Target gain
Disturbance torque	-126 dB	-100 dB
Angular rate	-33 dB	-30 dB
FOG error	15 dB	26 dB
Acceleration disturbance	-30 dB	-30 dB

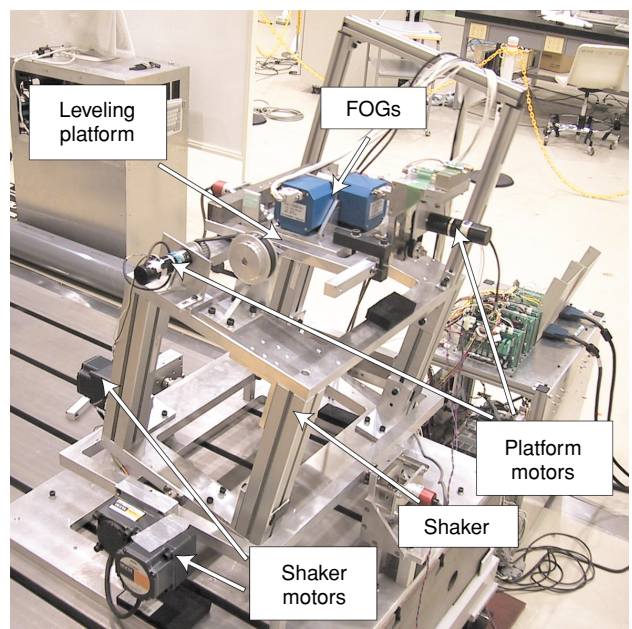


Fig. 11. Experimental equipment for leveling platform.

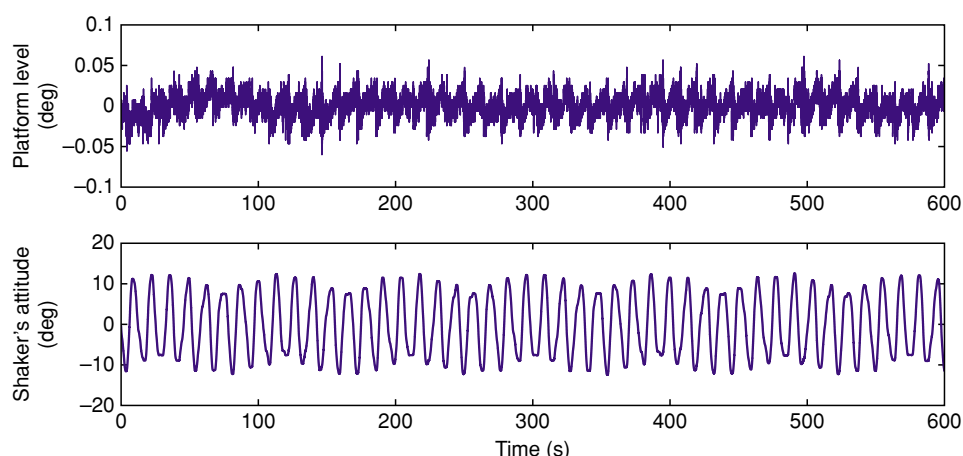


Fig. 12. Experimental results of leveling platform control.

Table 3. Controller design parameters of APM.

		Desirable	Undesirable
Step cycle	Long	Lower miscalculation rate	Slower response
	Short	Quicker response	Higher miscalculation rate
Step angle	Large	Lower miscalculation rate	Larger impact of miscalculation
	Small	Smaller impact of miscalculation	Higher miscalculation rate
Dithering amplitude	Large	Lower miscalculation rate	Larger impact on pointing error
	Small	Smaller impact on pointing error	Higher miscalculation rate

istics of the shaker's attitude were almost the same as the vessel's attitude shown in section 2. The experimental results showed that the platform level was maintained to within about  $0.05^\circ$  while being shaken. Thus, we demonstrated that this process could obtain an accurate controller.

### 5.3 Tracking controller design

A typical tracking control technique is the step-track concept [13] in which the signal levels of neighboring angles are compared. This concept is relatively simple: 1) the measured received signal level is integrated for a specific time (called a step cycle), 2) the present received level (A) is compared with the last received level (B), 3) if  $A > B$ , the antenna is rotated in the same direction by a small amount (called the step angle), if  $A < B$ , the antenna is rotated in the opposite direction by the step angle, and 4) steps 1 to 3 are repeated; this directs the antenna boresight to the maximum received level. The parameters of step-track design are:

- 1) step cycle
- 2) step angle.

Some desirable/undesirable tendencies versus the

parameter values are outlined in **Table 3**. A miscalculation means that the antenna is being driven in a direction that increases the pointing errors. It is clear that deciding each parameter's value involves a trade-off.

Step-track has a drawback: if the error angle per step cycle is larger than the step angle, the tracker cannot compensate for the pointing error. To offset this drawback, we introduced a dithering technique based on step-track. This technique always oscillates the APM conically: 1) the APM's pedestal continuously oscillates, (the oscillation amplitude is called the dithering amplitude, and the cycle is called the dithering cycle), 2) the measured signal level is integrated over half cycles, 3) the present level is compared with the level of the last half cycle, and the pedestal rotates by a small amount (called the step angle) in the direction in which the level is larger, and 4) steps 2 and 3 are repeated. The dithering design parameters are:

- 1) dithering amplitude
- 2) dithering cycle
- 3) step angle.

The sum of the dithering amplitude and step angle

must be smaller than the required pointing error angles.

Some desirable/undesirable tendencies for dithering amplitude design are shown in Table 3. The impacts of the dithering cycle and step angle on the control accuracy are the same as for the step cycle and step angle, respectively. Choosing each dithering parameter also involves trade-offs. The parameters are decided by trial and error using Table 3.

The tracking accuracy is highly dependent on the degree of signal fluctuation, which is caused by background noise and signal modulation. To moderate the signal fluctuation level, we can effectively apply a low pass filter (LPF) to the received signal. Using N-STAR [16] signals, we confirmed that fluctuations of  $\pm 1$  and  $\pm 2$  dB could be achieved with 300-Hz and 1-kHz LPFs, respectively. **Figure 13** shows the time simulation results for tracking accuracy using the step-track and dithering techniques when the leveling platform was swinging continuously at about  $0.05^\circ$  at 0.1 Hz. This motion is almost the same as for the leveling platform motion described in section 5.2.2.

As shown in Fig. 13, we clarified that dithering can achieve the required pointing accuracy when the fluctuation level is lower than  $\pm 2$  dB. On the other hand, step-track often fails.

## 6. Simulation results for entire antenna system

We carried out time simulations to evaluate the performance of the total antenna system. The system requirements demand that the antenna pointing error cannot exceed  $0.2^\circ$ , as described in section 2, under

the same disturbance and error conditions, using commercial sensors, as shown in Fig. 2 and Table 1. For the model parameters, we used the values of the prototype, as shown in Fig. 10.

We assumed that the distance from the vessel's rotation center to the antenna system's installation point was 10 m, signal fluctuation was  $\pm 1$  dB white noise, and the vessel was initially heading in the direction of the target satellite's azimuth. Hence, the APM El-axis was initially parallel to the platform's Y-axis and orthogonal to the platform's X-axis. The tracking control on the APM used only the El-axis. The vessel was accelerated to  $0.05 \text{ m/s}^2$  for 30–330 s, and its heading veered from  $0^\circ$  to  $90^\circ$  at a constant speed (about 30 knots) for 500–1100 s.

The simulation results for a conventional configuration using an accelerometer as the conventional inclinometer are shown in **Fig. 14**. The leveling platform was gradually tilted to counter low-frequency acceleration disturbances because the inclinometer miscalculates the acceleration as the platform inclines, and the controller inclines the platform to correct the angle to offset the measured acceleration. In this simulation, the translation acceleration disturbance (30–330 s) tilted the platform around its Y-axis, but the APM El-axis tracking compensated well for the Y-axis level/angle error. However, the turning motion degraded the pointing accuracy because the centrifugal acceleration induced by the turning tilted the platform around its X-axis, while the APM El-axis was orthogonal to the platform's X-axis at the initial moment of the turning motion. The El-axis's tracking control could not compensate for the X-

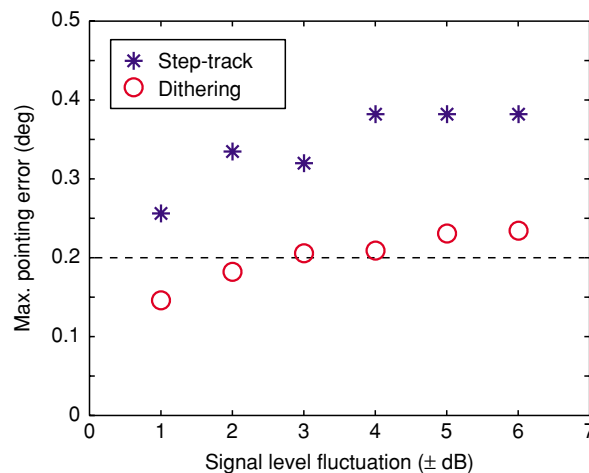


Fig. 13. Tracking accuracy of step-track and dithering.

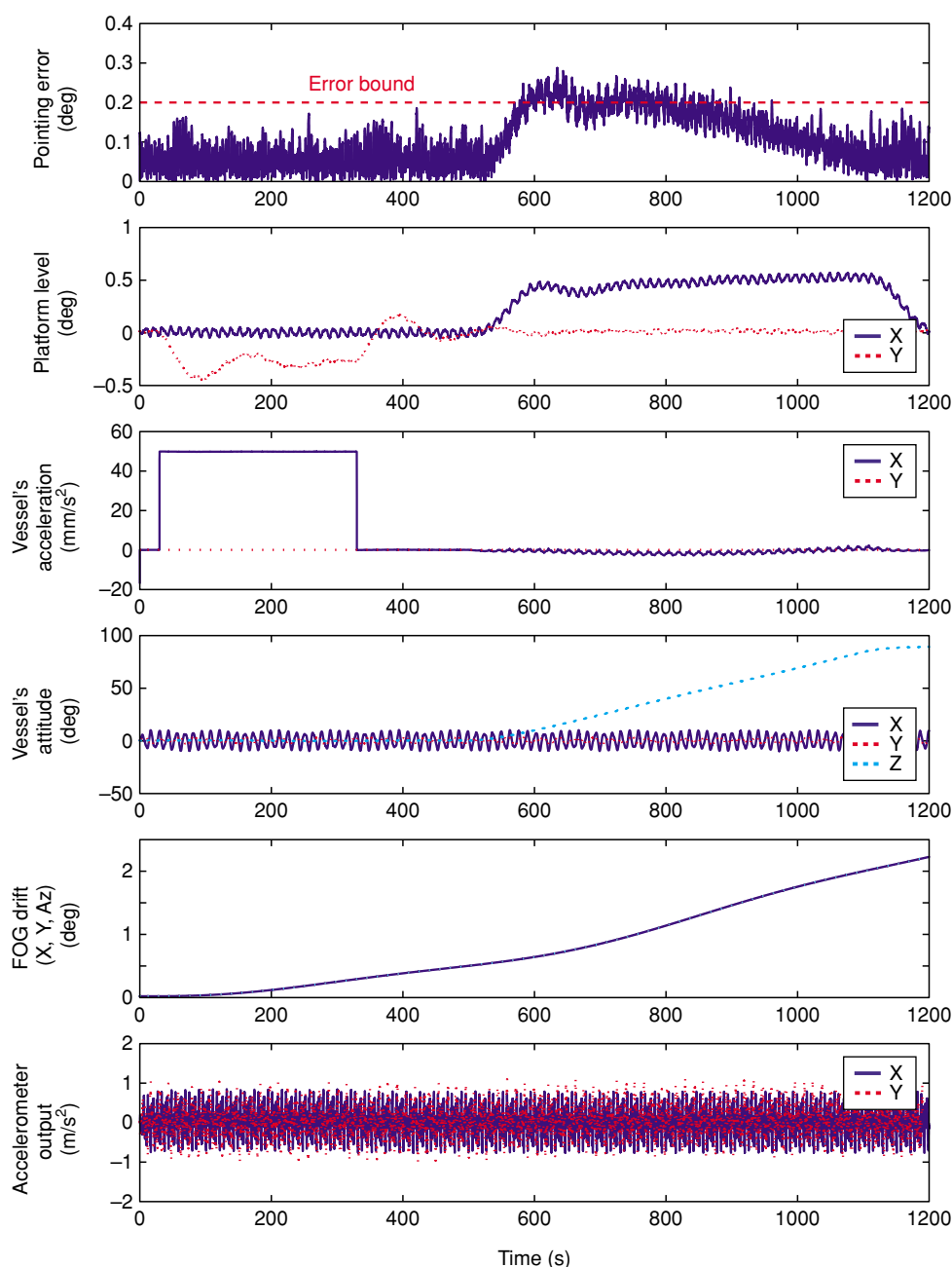


Fig. 14. Simulation results for conventional configuration.

axis's level/angle error.

The results obtained with our inclinometer are shown in **Fig. 15**. The platform level/angle was quite stable during the simulation, and we achieved a pointing accuracy of  $0.2^\circ$ . Thus, we confirmed the effectiveness of our inclinometer for low-frequency acceleration disturbances. Antenna systems using this inclinometer can meet ITU-R requirements.

These simulation results show that the system configuration, controllers, and new inclinometer enable

us to make a highly accurate pointing system at a low cost.

## 7. Conclusions

We described a highly accurate and cost-effective auto-tracking antenna system for earth stations onboard vessels, using a novel inclinometer that is highly accurate in acceleration disturbance environments and a new systematic stabilization controller

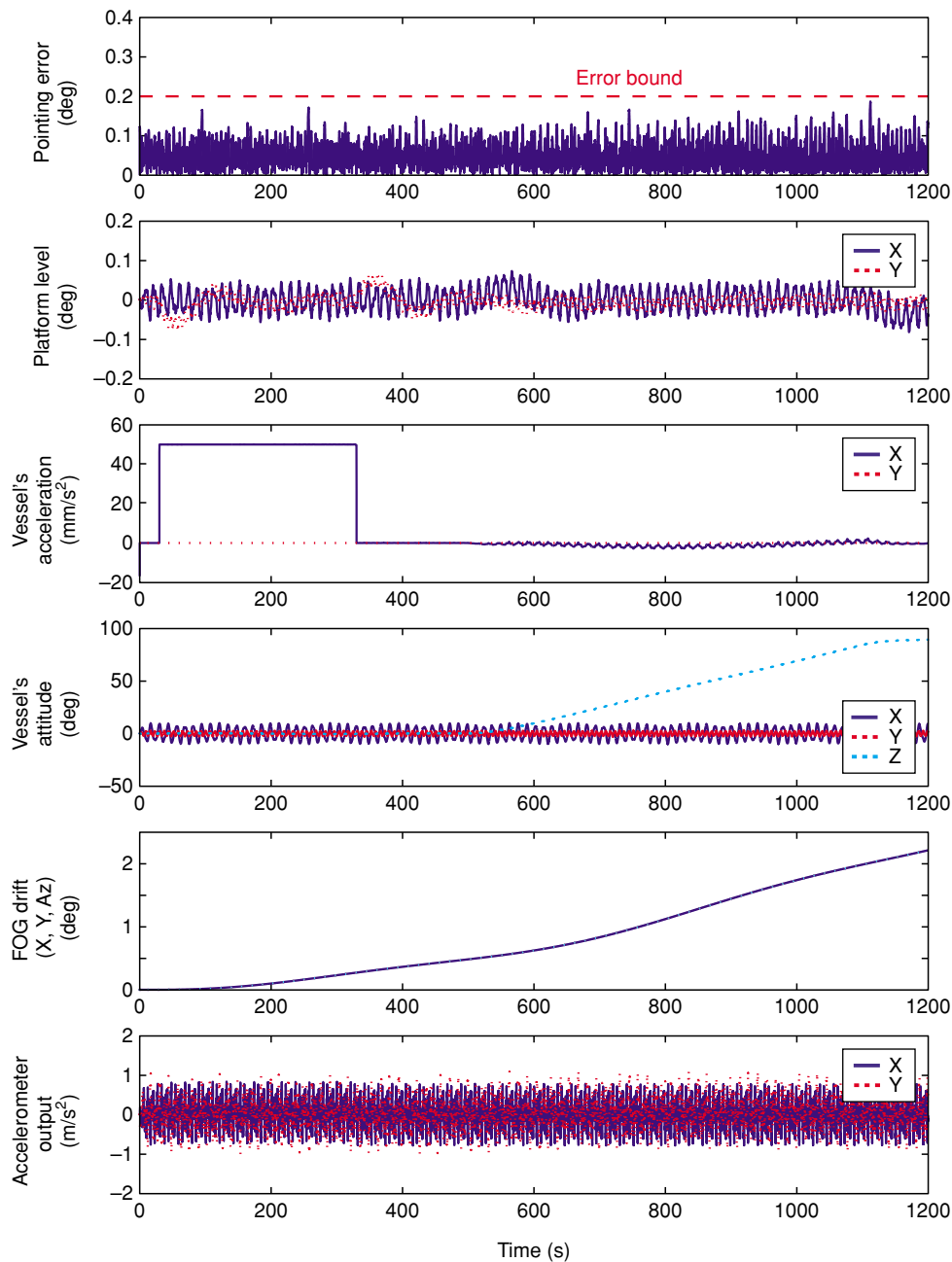


Fig. 15. Simulation results for proposed inclinometer.

design process to obtain the highly accurate controller with moderately accurate sensors. The antenna system consists of a leveling platform with an X-Y pedestal, an antenna pointing mechanism (APM) with an Az-El pedestal on the platform, and a reflector antenna with a single horn on the APM. Platform stabilization control is the key to achieving a highly accurate antenna system. One key technology for the leveling platform is the inclinometer, which was highly accurate, even in acceleration disturbance

environments, especially in long-term acceleration disturbance conditions, where conventional ones failed. Its configuration includes cost-effective accelerometers, a pendulum, and a rotary encoder. The second key technology is the design process that obtains highly accurate controllers using moderately accurate sensors, FOGs, and inclinometers. The process does not rely on the designer's skill and can avoid the interminable process of trial and error, so the design time is considerably shorter than for the

conventional process. The APM's tracking control was designed using the dithering technique. Finally, we performed an experimental evaluation of the stable platform and time simulations of the entire antenna system. The results clearly showed that the system could achieve its target pointing accuracy of  $0.2^\circ$ , even though low-cost sensors were used. We confirmed that this system configuration, the inclinometer, and the controller design process can achieve a high pointing accuracy and a low system cost.

## References

- [1] ITU-R Radio Regulations, Resolution 902, "Provisions Relating to Earth Stations Located on board Vessels which Operate in Fixed-Satellite Service Networks in the Uplink Bands 5 925–6 425 MHz and 14–14.5 GHz."
- [2] <http://www.inmarsat.com/>
- [3] T. Shiokawa, Y. Karasawa, and M Yamada, "Compact antenna systems for INMARSAT Standard-B ship earth stations," IEE 3rd International Conference on Satellite Systems for Mobile Communications and Navigation, London, UK, June 1983.
- [4] M. Taylor, "Higher Accuracy Direct Mechanical Stabilization for Marine SATCOM Antennas," AIAA 9th International Communications Satellite Systems Conference, 82-0530, pp. 512-519, 1982.
- [5] N. D. Dang, D. Pike, B. Claydon, and P. Crilley, "A Stabilised Satellite Terminal for Hostile Marine Environments," IEE 3rd European Conference on Satellite Communications, pp. 112-116, 2-4 Nov. 1993.
- [6] G. J. Hawkins and D. J. Edwards, "Operational Analysis of Electronic Tracking Schemes," IEE Proceedings I, Communications, Speech and Vision, Vol. 136, No. 3, pp. 181-188, June 1989.
- [7] T. Yoshida, K. Ohata, S. Ozawa, and M. Ueba, "High Accuracy Auto-Tracking Antenna System Using H-infinity Control for Earth Stations on board Vessels," AIAA Guidance, Navigation, and Control Conference, AIAA 2003-5731, 2003.
- [8] O. Lucke and M. Holzbock, "Antenna Agility Requirements and Pointing, Acquisition and Tracking for Broadband Mobile Satellite Terminals," AIAA 21st International Communications Satellite Systems Conference, AIAA 2003-2402, 2003.
- [9] C. L. Glennie, K. P. Schwarz, A. M. Bruton, R. Forsberg, A. V. Olsen, and K. Keller, "A comparison of stable platform and strapdown airborne gravity," Journal of Geodesy, Vol. 74, No. 5, pp. 383-389, 2000.
- [10] G. Harries and E. J. Stannard, "Design of a Small Shipborne Terminal ("SCOT")," IEE Proceedings of Conference on Earth Station Technology, No. 72, pp. 63-69, 1970.
- [11] J. V. Anders, E. F. Higgins, J. L. Murray, and F. J. Schaefer, "The Precision Tracker," Bell System Technical Journal, Vol. 42, pp. 1309-1356, 1963.
- [12] M. I. Skolnik, "Radar Handbook," McGraw-Hill, Chapter 21, 1970.
- [13] N. N. Tom and G. P. Heckert, "STEP-TRACK - A Simple Autotracking Scheme for Satellite Communication Terminals," AIAA 3rd Communications Satellite Systems Conference, No. 70-416, 1970.
- [14] K. Glover and J. C. Doyle, "State-Space Formulae for All Stabilizing Controllers that Satisfy an  $H_\infty$  Norm Bound and Relations to Risk Sensitivity," Systems and Control Letters, Vol. 11, pp. 167-172, 1988.
- [15] T. Iwasaki and R. E. Skelton, "All Controllers for the General  $H_\infty$  Control Problem: LMI Existence Conditions and State Space Formulae," Automatica, Vol. 30, No. 8, pp. 1307-1317, 1994.
- [16] K. Nakagawa, M. Minomo, M. Tanaka, and T. Itanami, "N-STAR: Communication Satellite for Japanese Domestic Use," AIAA 14th International Communications Satellite Systems Conference, AIAA-94-1078-CP, pp.1129-1134, 1994.



**Tomihiko Yoshida**

Engineer, Satellite Communication Service Development Project, NTT Access Network Service Systems Laboratories.

He received the B.E. and M.E. degrees in aerospace engineering from Nagoya University, Nagoya, Aichi in 1996 and 1998, respectively. He joined NTT Wireless Systems Laboratories, Kanagawa in 1998. He has been engaged in research on the dynamics of a large deployable satellite onboard antenna and auto-tracking antenna control systems for mobile satellite communication. He is a member of the Japan Society for Aeronautical and Space Sciences (JSASS) and the Institute of Electronics, Information and Communication Engineers (IEICE) of Japan.



**Kohei Ohata**

Senior Research Engineer, Supervisor, Satellite Communication Systems Group, Wireless Access Systems Project, NTT Access Network Service Systems Laboratories.

He received the B.E. and M.E. degrees in mechanical engineering from Keio University, Tokyo in 1981 and 1983, respectively. In 1983 he joined the Yokosuka Electrical Communication Laboratory, Nippon Telegraph and Telephone Public Corporation (now NTT). Since then, he has been engaged in R&D of satellite onboard antennas, earth station equipment, and satellite Internet systems. He is now focusing on R&D of the next-generation broadband mobile satellite communication system. He is a member of IEICE.



**Masazumi Ueba**

Senior Research Engineer, Supervisor, Group Manager of Satellite Communication Systems Group, Wireless Access Systems Project, NTT Access Network Service Systems Laboratories.

He received the B.E. and M.S. degrees in aeronautical engineering from the University of Tokyo, Tokyo in 1982 and 1984, respectively and the D.Eng. degree in 1996. In 1984, he joined the Yokosuka Electrical Communication Laboratories, Nippon Telegraph and Telephone Public Corporation (now NTT). He has been engaged in research on the dynamics of antenna pointing control systems of satellites and a shape control system for large antenna reflectors. He is currently engaged in research on technologies for the next-generation future mobile satellite communication system. He is a member of IEICE, JSASS, and the American Institute of Aeronautics and Astronautics.